VIROLOGY 232, 74–85 (1997)
ARTICLE NO. VY978553

A Specific Host Cellular Protein Binding Element Near the 3′ End

Qi Liu, Wei Yu,[1] and Julian L. Leibowitz[2]

Department of Pathology and Laboratory Medicine, Texas A&M University College of Medicine, 208 Reynolds Building, College Station, Texas 77843-1114

Received November 4, 1996; returned to author for revision November 27, 1996; accepted March 21, 1997

A distinct host cellular protein binding element was mapped within a 38-nucleotide (nt) sequence 166–129 nucleotides upstream of the 3′ end of the MHV-JHM genome using a RNase T_1 protection/gel mobility shift electrophoresis assay. The resultant RNA–protein complex contains six host cellular proteins, one protein of 120-kDa molecular mass, two poorly resolved species approximately 55 kDa in size, a second pair of poorly resolved 40-kDa proteins, and a minor component of 25 kDa. A series of RNA probes containing deletions or clustered transversion mutations were tested for their ability to form complexes with mock- and MHV-JHM-infected cytoplasmic extracts. Three mutant RNA probes (mA, mB, and mC) with deletions at 154–140, 139–129, and 128–118, respectively, expressed 4, 37, and 94% of the host protein binding activity exhibited by the wild-type RNA. Defective interfering (DI) RNAs (DImA, DImB, and DImC) containing corresponding deletions at 154–140, 139–129, 128–118, and another DI RNA (DImD) with a deletion at nucleotides (nts) 112–102, a region which did not affect RNA–protein interactions, were transfected into MHV-JHM-infected 17CL-1 cells to assay the effects of these mutations on DI RNA replication. All of these mutations had an adverse effect on DI RNA replication. However, analysis of negative strand mutant DI RNAs revealed that two mutants (DImC and DImD) carrying deletions having little or no effect on RNA–protein interaction in our RNA–protein binding assays maintained their mutant sequences. In contrast, the other two mutants (DImA and DImB) containing deletions that dramatically decreased RNA–protein binding activity did not maintain their mutations; wild-type sequences were restored in the majority of the progeny negative strand molecules. These data indicate that the 26-nucleotide sequence at positions 154–129 from the 3′ end of viral genome is important to both RNA–protein binding and viral replication. This protein binding element contains an 11-nt sequence (UGAGAGAAGUU, positions 139–129) very similar to a more 3′ sequence (UGAAUGAAGUU) previously implicated in host protein binding and viral RNA replication (Yu and Leibowitz, 1995a and 1995b).

INTRODUCTION

Coronaviruses are a widespread group of pathogens infecting many vertebrate species, including man (Siddell *et al.,* 1983; Wege *et al.,* 1982). Mouse hepatitis virus (MHV), the most extensively studied member of the coronavirus family, possesses an enveloped, single-stranded, plus-sense, genomic RNA approximately 31 kb in size (Lai and Stohlman, 1978; Lee *et al.,* 1991; Leibowitz *et al.,* 1990; Pachuk *et al.,* 1989). In MHV-infected cells, one genome-length and six subgenomic-sized mRNA species are synthesized. The largest RNA has been designated RNA 1 with the remainder of the subgenomic mRNA being numbered 2–7 in order of decreasing size. These RNAs comprise a 3′ coterminal nested-set, with the 5′ terminus of each mRNA containing a 70- to 80-nucleotide (nt) 5′ leader sequence identical to that present at the 5′ end of viral genome (Lai *et al.,* 1984; Leibowitz *et al.,* 1981; Spaan *et al.,* 1981).

Several different models have been proposed to explain MHV mRNA synthesis. In the leader-primed model, the full-length minus strand RNA is generated from the genomic RNA and serves as the template for the synthesis of virion RNA and subgenomic mRNAs. Free leader RNAs, synthesized from the 3′ end of the negative strand template, reassociate with the template at the intergenic region and serve as primers for the synthesis of subgenomic mRNA molecules (Lai, 1990). This model has been modified to incorporate the presence of subgenomic negative strand RNAs in the infected cells. After initial transcription of subgenomic mRNAs by the leader-primed mechanism, these mRNAs serve as templates for subgenomic negative strand synthesis; the subgenomic negative strands mRNAs than serve as templates for additional positive strands synthesis (Sethna *et al.,* 1989; Brian *et al.,* 1994). In the minus-strand template model, subgenomic negative strand RNAs are synthesized from the genome RNA and serve as the templates for subgenomic mRNA synthesis (Sawicki and Sawicki, 1990). In all of these models, synthesis of minus-strand RNAs is an indispensable first step in viral RNA replication.

The extremely large size of the MHV genome has, to

[1] Current address: Department of Molecular and Human Genetics, Baylor College of Medicine, One Baylor Plaza, Houston, TX 77030.

[2] To whom correspondence and reprint requests should be addressed. Fax: (409) 862-1299. E-mail: jleibowitz@tamu.edu.

0042-6822/97 $25.00

date, precluded utilizing a reverse genetic approach to study replication of the genomic RNA. However, this obstacle has been partially overcome by utilizing replication competent defective interfering (DI) RNAs as model replicons (Makino *et al.,* 1991). Deletion analyses of naturally occurring MHV-JHM DI RNAs show that 474 nucleotides from the 5′ end of genomic RNA, 436 nt from the 3′ end of the genome, and 57 nt in an internal position from nt 3218 to 3274 at the 5′ end of the genome contain crucial cis-acting signals for DI RNA replication in the presence of helper virus (Kim *et al.,* 1993; Lin and Lai, 1993; Makino *et al.,* 1988; Kim and Makino, 1995). Modest-sized deletions of either the 5′ or 3′ cis-acting elements are able to destroy the ability of synthetic DI RNA to replicate. One study has utilized a DI RNA to investigate the cis-acting signal for MHV minus-strand RNA synthesis. The poly(A) tail and only 55 nucleotides from the 3′ end of the MHV genome upstream from the poly(A) tail were required for the synthesis of minus strand RNA (Lin *et al.,* 1994).

We have been studying MHV replication by precisely identifying the cis-acting signals for RNA synthesis and the proteins which recognize these signals at the 3′ end of MHV genomic RNA. Recently, utilizing RNase T_1 protection/gel mobility shift electrophoresis, we reported the specific binding of host cellular proteins to two distinct sites within the 3′ end of MHV-JHM genomic RNA (Yu and Leibowitz, 1995a). One site was mapped within the 3′ most 42 nt of the genomic RNA, and designated 3′(+) 42. A second upstream site was mapped to nucleotides 171–85 upstream from the 3′ end of the viral genome. Comparison of the two protein binding elements revealed the presence of 11-nt UGARNGAAGUU motif, which is conserved among all MHV strains (Parker and Masters, 1990). Mutational analysis of the 3′ (+) 42 sequence demonstrated that a 19-nt sequence spanning position 42–24 nucleotides upstream of the 3′ end of genomic RNA was required for host protein binding. The conserved 11-nt motif, UGAAUGAAGUU, within 3′ (+) 42 was essential for both host protein binding and viral RNA replication (Yu and Leibowitz, 1995b).

In the current work, we precisely map the second protein binding element to a 38-nucleotide sequence encompassing nucleotides 166–129 upstream of the 3′ end of the MHV-JHM genome, again using the RNase T_1 protection/gel mobility shift electrophoresis assay. A series of RNA probes containing deletions or clustered-point mutations within this 38-nt sequence were tested for their ability to form complexes with mock- and MHV-JHM-infected cytoplasmic extracts. DI RNAs carrying deletions within or beyond this specific element were constructed to investigate its role in viral RNA replication. Our data indicates that sequences encompassed by nt 154–129 within this protein binding element are involved in viral replication. The conserved 11-nt motif (UGAGAGAAGUU) at nt 129–139 plays an important role in both viral RNA replication and host cellular protein binding.

MATERIALS AND METHODS

Viruses and cells

MHV strain JHM and murine 17CL-1 cells were grown as previously described (Leibowitz *et al.,* 1981). The JHM strain of MHV was used as a helper virus throughout this study.

PCR

PCR was conducted to synthesize cDNA fragments representing various specific regions near the 3′ end of viral genome. The 5′ end positive sense primers all contained the sequence 5′-TAA TAC GAC TCA CTA TAG GGC GAG-3′ (pT7) to put the cDNAs under the control of the T7 RNA polymerase promoter. The primer pairs used are listed in Table 1. Linearized plasmid DE25, a 2.2-kb cDNA derived from DIssE RNA, was used as the template in PCR reactions. To synthesize mutant cDNA fragments, a variety of clustered-point mutations and deletions were introduced into either the 5′ end or 3′ end primers. Overlapping primer pairs were also adopted for nontemplate PCR. Identical conditions were used for amplifying all fragments subsequently used as transcription templates. Amplification was performed at 95° for 60 sec, 50° for 30 sec, 72° for 90 sec for 10 cycles, at 95° for 30 sec, 55° for 30 sec, 70° for 60 sec for the next 10 cycles, at 95° for 30 sec, 70° for 60 sec for the last 10 cycles, followed by a 5-min extension at 72° in a MiniCycler (MJ Research). PCR products were resolved by gel electrophoresis through 2–3% BIOGEL agarose (Bio 101) and recovered from gel slices using the Mermaid kit (Bio 101).

In vitro RNA transcription and radiolabeling

PCR products were used as templates for *in vitro* transcription of radiolabeled RNA probes with T7 RNA polymerase as described previously (Yu and Leibowitz, 1995a).

RNase T_1 protection/gel mobility shift electrophoresis and UV induced cross-linking

Mock- and MHV-JHM-infected cytoplasmic extracts of 17CL-1 cells were incubated with 2 ng of [^{32}P]UTP-labeled probe at 22° for 20 min, followed by limited digestion with RNase T_1 at 22° for 20 min (Yu and Leibowitz, 1995a). Ten micrograms of heparin (Sigma) and 500 ng of poly (I)-poly (C) (Boehringer Mannheim) were included in each binding reaction to decrease nonspecific binding. RNase T_1 titration was carried out to select the optimal RNase T_1 concentration for each probe; a RNase T_1 concentration of 0.00625 units per reaction was found to be optimal for all probes used in this study. RNA–protein

TABLE 1

Probes and Primers Synthesized

Probe	Positive-sense 5′ primers[a]	Negative-sense 3′ primers[a]
171-85	pT7-TTA GTT GAA AGA GAT TGC	GGG CGC CTA TCG CCG TT
166-85	pT7-GAA AGA GAT TGC AAA ATA GAG	GGG CGC CTA TCG CCG TT
154-85	pT7-AAA ATA GAG AAT GTG TGA GAG	GGG CGC CTA TCG CCG TT
113-85	pT7-TCT AAC CAT AAG AAC GGC	GGG CGC CTA TCG CCG TT
171-118	pT7-TTA GTT GAA AGA GAT TGC	GGA CCT TGC TAA CTT CTC TCA CAC ATT CTC TAT TTT
166-118	pT7-GAA AGA GAT TGC AAA ATA GAG	GGA CCT TGC TAA CTT CTC TCA CAC ATT CTC TAT TTT
mA	pT7-GAA AGA GAT TGC^TGA GAG AAG TTA GCA AGG	GGG CGC CTA TCG CCG TT
mB	pT7-GAA AGA GAT TGC AAA ATA GAG	GGG CGC CTA TCG CCG TTC TTA TGG TTA GAC GTA GGA CCT TGC T^CACAT TCT CTA TTT TGC AAT CTC TTT C
mC	pT7-GAA AGA GAT TGC AAA ATA GAG	GGG CGC CTA TCG CCG TTC TTA TGG TTA GAC GT^A ACT TCT CTC ACA CAT TCT CTA TTT TGC AAT CTC TTT C
mE	pT7-CTT TCT CTA ACC AAA ATA GAG-AAT GTG TGA G	GGG CGC CTA TCG CCG TT
mF	pT7-GAA AGA GAT TGG TTT TAT CTC TAT GTG TGA GAG	GGG CGC CTA TCG CCG TT
mG	pT7-TTA GTT GAA AGA GAT TGC	GGA CCT TGC TTT GAA GAG AGT CAC ATT CTC TAT TTT

[a] The underlined nucleotides indicate transversions from the wild-type sequence found in DE25. The ^ symbols in mA, mB, and mC indicate that wild-type sequences have been deleted, as described under Materials and Methods.

complexes were resolved by electrophoresis through a 6% polyacrylamide nondenaturing gel at 200V for 3 hr at 4° (Yu and Leibowitz, 1995a). The RNA–protein binding activity was quantitated using a phosphoimager (Molecular Dynamics Inc). The protocols for labeling host polypeptides bound to RNA probes by UV cross-linking assays have been reported elsewhere (Yu and Leibowitz, 1995a).

Construction of mutant DI plasmids

Plasmid DE25, derived from the MHV-JHM DIssE RNA (Makino *et al.,* 1988; Makino and Lai, 1989), served as the target template to construct mutant plasmids using the Chameleon double-stranded, site-directed mutagenesis kit (Stratagene) following the manufacturer's recommended procedures. The selection primer (5′-GCG CGA GGC CCA GAA CGT TAA TAC GAC TCA CTA TAG-3′) destroys the unique *Hin*dIII restriction site upstream of the 5′ end of DE25 (Makino and Lai, 1989). The mutagenic primers contained a set of deletions within the 3′ end of viral genome. Mutagenic primer A (5′-GTT GAA AGA GAT TGC TGA GAG AAG TTA GCA-3′) contains a 15-nt deletion spanning nt 154–140 upstream of the 3′ end of the viral genome. Mutagenic primer B (5′-AAA ATA GAG AAT GTG AGC AAG GTC CTA CGT-3′) contains an 11-nt deletion from nt 139 to 129. Mutagenic primer C (5′-GTG TGA GAG AAG TTA CGT CTA ACC ATA AG-3′) contains an 11-nt deletion at nt 128–118. Mutagenic primer D (5′-GTT AGC AAG GTC CTA CGT AAC GGC GAT AGG CGC CCC-3′) contains an 11-nt deletion from nt 112 to 102. PCR was utilized to screen bacteria carrying mutant plasmids. Briefly, bacterial colonies were randomly picked and dispersed into 5 μl of 2xYT media. One microliter of the suspension was used as a template for PCR and the remainder was stored at 4°. The 5′-positive sense primer (GAA GGT TGT GGC AGA CCC TG) is complementary to negative strand DNA at nt 2018 to 2038 from the 5′ end of DE25 cDNA (corresponding to positions 198–178 upstream from the 3′ end), the 3′ negative sense primer (GGG CGC CTA TCG CCG TT) is complementary to positive strand DNA at nt 85 to 101 from the 3′ end DE25 cDNA. PCR was carried out under conditions identical to those employed to amplify fragments used as transcription templates. The primers used for site-directed mutagenesis are summarized in Table 2. Mutant DI plasmids were distinguished from wild type by electrophoresis of the resulting PCR products through 3–4% Metaphor (FMC) agarose gels. Once bacterial colonies carrying the mutation were identified, they were grown in 2xYT media at 37° overnight, and plasmid DNAs were purified using the Prep-A-Gene DNA purification kit (Bio-Rad). Purified DNA was sequenced to confirm the presence of the introduced mutations and to verify that no additional mutations were introduced into the plasmids.

DI RNA transfection

Plasmid DNAs linearized by *Xba*I digestion were transcribed *in vitro* by T7 RNA polymerase using the mCAP capping kit (Stratagene). T7 RNA transcripts were treated with 4 U of RNase-free DNase (Stratagene) at 37° for 15 min, extracted twice with phenol/chloroform, and purified by gel filtration over a G-50 column. Transfection of DI RNAs was performed according to procedures previously published (Yu and Leibowitz, 1995b). DI RNA (1.5 μg) was mixed with 15 μg of cellFECTIN (Life Technologies) at room temperature for 15 min and then at 1 hr postinfection transfected into MHV-JHM-infected murine 17CL-1 cells in a 35-mm dish.

TABLE 2

Probes and Primers Used for Site-Directed Mutagenesis and RT-PCR

Primer use	Primers sequence
Mutagenic primer A (for DImA)	GTT GAA AGA GAT TGC TGA GAG AAG TTA GCA
Mutagenic primer B (for DImB)	AAA ATA GAG AAT GTG AGC AAG GTC CTA CGT
Mutagenic primer C (for DImC)	GTG TGA GAG AAG TTA CGT CTA ACC ATA AG
Mutagenic primer D (for DImD)	GTT AGC AAG GTC CTA CGT AAC GGC GAT AGG CGC CCC
Selection primer	GCG CGA GGC CCA GAA CGT TAA TAC GAC TCA CTA TAG
5′ Screening primer	GAA GGT TGT GGC AGA CCC
3′ Screening primer	GGG CGC CTA TCG CCG TT
Reverse transcription primer/5′ PCR primer	GGC GTT GTC TAA AGA GAT TTG
3′ PCR primer	GTG ATT CTT CCA ATT GGC
5′ Nested PCR primer	GAA GGT TGT GGC AGA CCC TG
3′ Nested PCR primer	GGG CGC CTA TCG CCG TT

Detection of positive strand DI RNA replication by agarose gel electrophoresis

Intracellular RNA was labeled with 200 μCi/ml ^{32}Pi (ICN) from 7.5 to 9.5 hr postinfection in the presence of 10 μg/ml actinomycin D and 2% dialyzed FBS. Total RNA was isolated by extraction with 8 *M* guanidium hydrochloride (Yu and Leibowitz, 1995b). One-third of the total RNA sample was used for positive strand RNA analysis, and two-thirds was used for analysis of negative strand RNA. Positive strand RNA was resolved by 1% agarose gel electrophoresis in MOPS and formaldehyde at 100V for 6 hr. The gel was fixed with 80% methanol, dried, and exposed to X-ray film. Relative replication efficiency was quantitated with a phosphoimager (Molecular Dynamics Inc).

RT-PCR analysis of negative-strand RNA

To avoid detecting the helper virus, the reverse transcription primer (5′-GGC GTT GTC TAA AGA GAT TTG-3′, which anneals to negative strand DI RNA at position 1601–1621 from the 5′ end) was chosen to span the junction region between domain II and domain III of DE25 (Makino *et al.,* 1988). Reverse transcription was performed as previously described (Yu and Leibowitz, 1995b). Synthesized cDNA was then used as a template for PCR. The 5′ positive sense primer for PCR was identical to that used for reverse transcription. The 3′ negative sense primer, 5′-GTG ATT CTT CCA ATT GGC-3′, is complementary to the last 18 nucleotides at the 3′ end of positive sense DE25 cDNA. cDNA fragments around 615–600 bp were amplified by 30 cycles of PCR (95° for 1 min, 51° for 30 sec, 72° for 90 sec, with the last extension at 72° for 5 min).

Nested PCR was conducted to detect the presence of deletions in negative-strand DI RNAs. The 615–600-bp PCR products were displayed by electrophoresis through a 1% agarose gel (SEAKEM GTG). DNA fragments were recovered from the gel slices using a GeneClean II kit (Bio 101 Inc.) and then used as templates for nested PCR. The sequence of the 5′ positive sense primer was 5′-GAA GGT TGT GGC AGA CCC TG-3′, that of the 3′ negative sense primer was 5′-GGG CGC CTA TCG CG TT-3′. The primer pairs were designed to flank the region containing introduced deletions and amplify a fragment encompassing nt 198–85 upstream from the 3′ end of the viral RNA genome. The conditions used for nested-PCR were identical to those used to generate cDNAs near the 3′ end of the viral genome. Mutants carrying the deletions were distinguished from wild type by gel electrophoresis through 3.5–4% MetaPhor agarose (FMC) at 100V for 3 hr.

RESULTS

Mapping the RNA sequence required for host cellular protein binding

Previous studies have demonstrated that a 87-nt sequence encompassing nt 171–85 upstream from the 3′ end of the MHV genome binds to host cellular proteins (Yu and Leibowitz, 1995a). To better define the boundaries of the essential sequences within this protein binding site, a set of RNA probes with deletions at either 5′-, 3′-, or both ends were transcribed from corresponding PCR templates to test their ability to form RNA–protein complexes with extracts prepared from uninfected cells. In the first series of experiments we compared the protein binding activities of probes, which were shortened from position 85 to position 118 at the 3′ end, from position 171 to position 166 at the 5′ end, or truncated at both the 5′ and 3′ ends. As shown in Fig. 1A, the 166–85 probe exhibited 116% of the host protein binding activity as did the 171–85 probe. Deletion of 3′ sequences (probe 171–118) did not decrease binding activity compared to the 171–85 probe, rather it resulted in a slight increase in binding activity (110%). Deletion of both 3′ and 5′ sequences in the 166–118 probe did not significantly decrease binding activity compared to the 171–85 probe. Thus this set of truncations mapped the

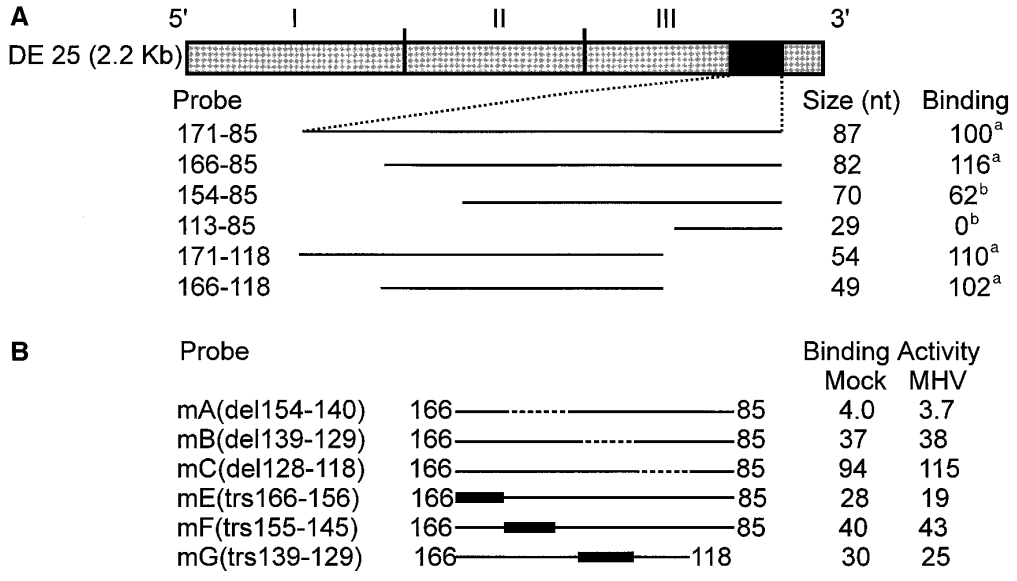

FIG. 1. Schematic diagram of DE25 cDNA, the locations of RNA probes, and summary of RNase T_1 protection/gel mobility shift electrophoresis assays. (A) RNA probes were radiolabeled and transcribed from the corresponding PCR-synthesized cDNA fragments. Each probe was named by its location within the genomic RNA sequence upstream from the 5′-most A in the poly(A) tail (position 0). For example, the probe 171–85 represents a 87-nt sequence extending from nt 171 to nt 85 upstream from position 0. The size of each probe is indicated in the figure, as is the relative protein binding activity. The amount of radioactivity in RNase T_1-resistant complexes for each probe was determined using a phosphoimager. To calculate relative protein binding activities of truncated probes, the amount of label was compared with a standard probe which was either the 171–85 probe (indicated by [a]) or the 166–85 probe (indicated by [b]). (B) The effect of mutations on RNA–protein interaction. Two sets of mutants (deletion and clustered transversions) were assayed to test their abilities to form RNA–protein complexes. The protein binding activities of mutants were quantitated by comparison to their corresponding wild-type RNAs. mA, mB, and mC are deletion mutants; mE, mF, and mG are transversion mutants. The sites of the mutations are listed in the parentheses. For example, del154–140 represents the deletion of 15 nt from nt 154 to nt 140 upstream from the 5′-most A in the poly(A) tail (position 0); trs166–156 represents the transversion of 11 nt from nt 166 to nt 156 upstream from the 5′-most A in the poly(A) tail (position 0).

protein binding element within nucleotides 166–118. Two additional probes with 5′ truncations were constructed to further map the protein binding element. The results we obtained with these two additional probes are also summarized in Fig. 1A. The protein binding activity of a 154–85 probe was 62% of that observed with 166–85, while the 113–85 RNA probe did not have any protein binding activity in our assay. Taken together these two experiments indicated that 49 nt corresponding to nt 166 to 118 upstream from the 3′ end of the RNA genome are sufficient to mediate RNA–host protein binding. Similar results in binding assays were obtained using extracts from MHV-infected and uninfected cells (data not shown).

To verify the specificity of this RNA–protein binding element, competition experiments with a 200-fold molar excess of unlabeled specific competitor RNA and nonspecific tRNA were performed. As shown in Fig. 2, two specific RNA–protein complexes were observed. They behaved identically in competition experiments. Excess unlabeled specific 166–118 RNA almost completely blocked the RNA–protein interactions (lanes 3 and 6), while the same amount of tRNA hardly affected the formation of RNA–protein complexes (lanes 4 and 7). No radioactivity was present in the gel when 166–118 probe was digested by RNase T_1 in the absence of cytoplasmic extract (lane 1). A comparison of the RNA binding activity exhibited by extracts derived from infected and uninfected cells revealed no significant differences (lanes 2 and 5).

A conserved 11-nt motif at position 139–129 upstream from the 3′ end MHV genome (UGAGAGAAGUU) is included in the 166–118 protein binding sequence. This motif has been demonstrated to be an important component of a more 3′ protein binding element. To assay the contribution of this 11-nt motif to RNA–protein interactions, we transcribed two types of mutant riboprobes and compared their protein binding ability to that of wild-type RNA probes. A set of deletions (mA, mB, and mC) produced dramatically different effects on RNA–protein interactions (Figs. 1B and 3). The RNA probe with a 15-nt deletion (mA) spanning nt 154–140 reduced host protein binding to 4% of wild type, the probe with a 11-nt deletion (mB) from nt 139–129 displayed 37% of wild-type binding activity, whereas the probe with a 11-nt deletion (mC) at nt 128–118 maintained 94% of the wild-type binding activity. A second class of mutants containing 11 nt clustered transversion mutations at nt 166–156 (mE), nt 155–145 (mF), and nt 139–129 (mG), decreased *in vitro* binding of host protein to RNA to 28, 40, and 30%, respectively, of that observed with wild-type RNA probes (Fig. 1B). Taken together, these data revealed that the 38 nucleotides from nt 166 to 129 all contribute to host cellular

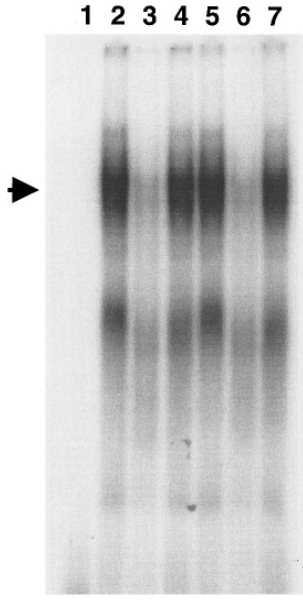

FIG. 2. Specific binding of mock- and MHV-JHM-infected cytoplasmic extracts to the wild–type 166–118 RNA. RNA–protein binding reactions were performed as described under Materials and Methods except that a 200-fold molar excess of unlabeled specific 166–118 RNA (lanes 3 and 6) and tRNA (lanes 4 and 7) were added to the reaction tubes prior to mixing the [^{32}P]UTP-labeled 166–118 riboprobe with mock-infected (lanes 2–4) or MHV-JHM-infected (lanes 5–7) cytoplasmic extracts. The binding mixtures underwent limited digestion with RNase T_1 and RNA–protein complexes were resolved as described under Materials and Methods. Lane 1 contained the 166–118 riboprobe thus treated in the absence of cytoplasmic extracts. The arrowhead indicates the position of the RNA–protein complex.

protein binding. The conserved 11-nt motif (nt 139–129) previously implicated in protein binding at a more downstream site lies within this protein binding element.

Identification of RNA binding proteins by UV induced cross-linking

UV-induced covalent cross-linking was carried out in solution to identify proteins which interact with this protein binding site. Mock- and JHM-infected cellular cytoplasmic extracts were incubated with *in vitro*-transcribed RNA probes under the same conditions used for RNA–protein binding assays. After limited digestion with RNase T_1 the RNA–protein complexes were cross-linked by UV irradiation. The cross-linked complexes were then completely digested by RNase A and resolved by SDS–PAGE. The protein profiles are shown in Fig. 4. The RNA–protein complex formed with 166–85 or 154–85 RNA contains six labeled polypeptides, a clearly defined 120-kDa band, two poorly resolved species around 55 kDa, a second pair of poorly resolved proteins around 40 kDa, and a minor component at 25 kDa. The RNA–protein complexes observed with MHV-JHM-infected cell lysate and mock-infected cell lysate were indistinguishable. When cell lysate was omitted from RNA–protein binding reaction, no labeled bands were detected. Results obtained by UV cross-linking correlated with those obtained in RNase T_1 protection/gel mobility shift assays. Virtually no labeled polypeptides were observed when cell lysate was incubated with the mA probe which possessed only 4% of the protein binding activity observed with wild-type probe. Attempts to separately determine the protein composition of the two RNA–protein complexes formed (Fig. 2) by *in situ* cross-linking or by purifying these complexes prior to cross-linking were unsuccessful.

The effect of mutation of the protein binding elements on DI RNA replication

The availability of a synthetic DI RNA replicon allowed us to examine the effect of mutations within the 166–129 protein binding element on MHV replication. A series of deletion mutant DI cDNAs were constructed from the wild-type DE25 template by site-directed mutagenesis. These mutants corresponded to the mutations tested in RNA–protein binding assays. Corresponding mutant DI RNAs were transcribed *in vitro* and transfected into 17CL-1 cells infected with MHV-JHM as helper virus. Positive strand DI replication was measured by gel electrophoresis after metabolic labeling with [^{32}P]orthophosphate in the presence of actinomycin D. In three independent experiments, after transfection with DImA RNA containing a 15-nt deletion from nt 154 to 140 from the 3′ end of viral genome, the synthesis of positive strand DI RNA was 24 to 65% observed after transfection with wild-type DE25 RNA. After transfection with DImB RNA, which carried a complete deletion of the 11-nt motif at 139–129, newly synthesized positive strand DI RNA was undetectable in all of the three separate experiments. One such experiment is shown in Fig. 5A. RT-PCR was employed to investigate negative strand DI RNA synthesis and to determine if the introduced mutations had been maintained during replication. As shown in Fig. 5B, negative strand RNA could always be detected in cells transfected with either DImA (lane 3) or DImB (lane 4) RNA, even though the corresponding positive strand RNA was undetectable for DImB. This held true in three independent experiments. Since recombination is a frequent event during MHV infection, a second PCR using primers flanking the deletions was carried out to determine if replicating minus-strands still contained the deletions. DE25 cDNA and mutant cDNAs constructed by site-directed mutagenesis were used as templates for nested-PCR to provide size markers for the wild-type and mutant DI RNAs. As shown in Fig. 5C, only a small fraction of the nested PCR products contained the introduced deletions (lanes 5 and 6), the majority of the progeny negative strand molecules yielded PCR products indistinguishable from wild type. In one experiment, the original, approximately 600-nucleotide, RT-PCR product was gel purified and subjected to automated sequencing. This confirmed

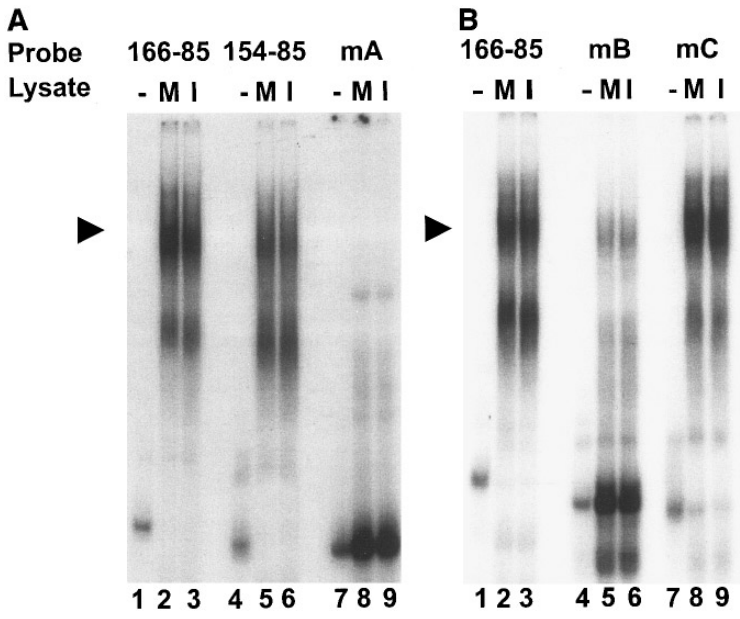

FIG. 3. Deletion mapping of RNA sequences contributing to protein binding. RNA–protein binding reactions were carried out as described under Materials and Methods. The mA probe contains a 67-nt sequence from 166 to 85 with a 15-nt deletion at 154–140 from the 3′ end of the viral genome; the mB probe contains a 71-nt sequence from 166 to 85 with a 11-nt deletion at 139–129; the mC probe contains a 71-nt sequence from 166 to 85 with a 11-nt deletion at 128–118. The arrowheads indicate the positions of the RNA–protein complexes. (A) Lanes 1, 4, and 7, 166–85, 154–85, and mA probes assayed without cytoplasmic extracts, respectively; lanes 2, 5, and 8, 166–85, 154–85, and mA probes incubated with mock-infected cytoplasmic extracts, respectively; lanes 3, 6, and 9, 166–85, 154–85, and mA probes incubated with MHV-JHM-infected cytoplasmic extracts, respectively. (B) Lanes 1, 4, and 7, 166–85, mB, and mC probes without cytoplasmic extracts, respectively; lanes 2, 5, and 8, 166–85, mB, and mC probes incubated with mock-infected cytoplasmic extracts, respectively; lanes 3, 6, and 9, 166–85, mB, and mC probes incubated with MHV-JHM-infected cytoplasmic extracts, respectively.

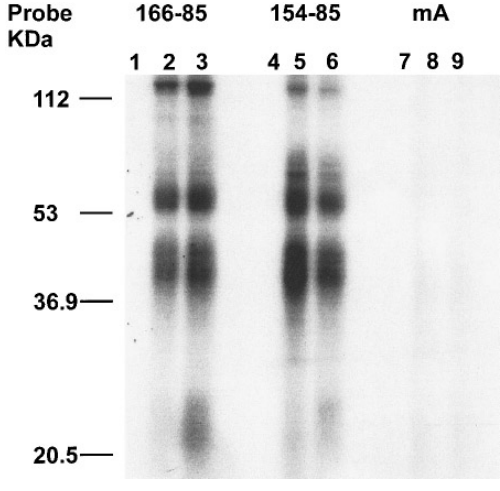

FIG. 4. Labeling of mock- and MHV-JHM-infected cellular proteins by UV cross-linking. After performing RNA–protein binding reactions as described under Materials and Methods, the reaction mixtures were exposed to UV light for 30 min and then completely digested with RNase A. Labeled proteins were resolved by 12% SDS–polyacrylamide gel electrophoresis and visualized by autoradiography. Prestained molecular weight standards (Bio-Rad) were used as markers. Lanes 1, 4, and 7, 166–85, 154–85, and mA probes in the absence of cell lysates; lanes 2, 5, and 8, 166–85, 154–85, and mA probes incubated with mock-infected cell lysates; lanes 3, 6, and 9, 166–85, 154–85, and mA probes incubated with MHV-JHM-infected cell lysates.

that the mutations introduced into DImA and DImB were replaced by the wild-type sequence. Presumably, the majority of the molecules which did not contain the introduced deletions arose by recombination with helper virus.

We next investigated the effect of two additional mutations, mC (del 128–118) and the deletion of nucleotides 112–102, on DI replication. These two deletion mutations had little and no effect on RNA–protein interaction in our RNase T_1 protection/gel mobility shift electrophoresis assay (Fig. 1A, probes 171–118 and 165–118; Fig. 1B, probe mC). Deletion mutant DI cDNAs were constructed from wild-type DE25 template by site-directed mutagenesis and the corresponding DI RNAs, DImC and DImD, synthsized by *in vitro* transcription. In replicate experiments, one of which is shown in Fig. 6, DImC and DImD replicated to 4 and 49%, respectively, as well as wild-type DE25. Analysis of negative strand DI RNAs by RT-PCR and nested PCR revealed that the mutations in DImC and DImD were maintained (Figs. 6B and 6C). In one experiment, the original, approximately 600-nucleotide, RT-PCR product was gel purified and subjected to automated sequencing. This confirmed that the mutations introduced into DImC and DImD were maintained.

DISCUSSION

In this study we have more precisely defined the RNA sequence requirements for binding host and/or viral pro-

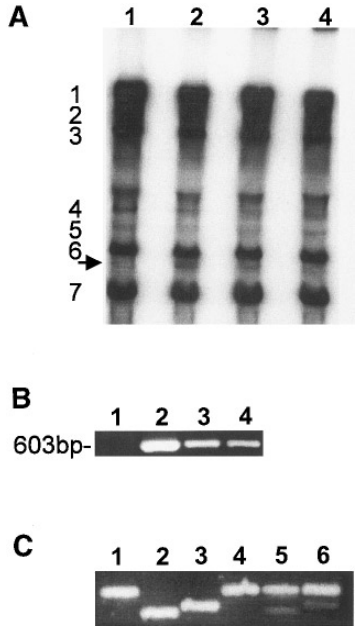

FIG. 5. Replication of wild–type DE25 and DE25-derived mutants DImA and DImB in MHV-JHM-infected cells. *In vitro*-transcribed DI RNA was transfected into MHV-JHM-infected 17CL-1 cells as described under Materials and Methods. Intracellular RNA was labeled with ^{32}Pi from 7.5 to 9.5 hr postinfection in the presence of actinomycin D and isolated with guanidium hydrochloride. (A) Equal amounts of each sample (2.5 μg) were electrophoresed in a 1% agarose gel containing MOPS and formaldehyde. For each sample, the amount of radioactivity migrating at the position of DI RNA, indicated by the arrow, was determined with a phosphoimager. The amounts of DImA and DImB RNA synthesized relative to DE25 RNA were calculated and are reported in the text. Lane 1, MHV-JHM-infected intracellular RNA without transfected DI RNA; lane 2, transfected with DE25; lane 3, transfected with DImA; lane 4, transfected with DImB. (B) cDNAs were synthesized from intracellular RNA by reverse transcription using a primer which spans the junction of DI regions II and III and thus only primes synthesis from negative strand DE25 RNA template. After PCR, a cDNA fragment around 600–615 bp was displayed by 1% agarose gel electrophoresis. Lane numbers correspond to the same samples as for A. A ϕX174 DNA/HaeIII fragment was used as a 603-bp size marker. The amplified DNA fragments around 600–615 bp shown in B were recovered and used as templates for the amplification of smaller fragments containing the mutagenized regions in the input DI RNAs. The plasmids used for transcription of wild-type and mutant DI RNAs were also used as templates for nested PCR to provide size markers for the expected wild-type and mutant sequences. PCR products were resolved by 3.5% Metaphor agarose gel electrophoresis. Lanes 1, 2, and 3, plasmids DE25, mA, and mB, respectively, were used as templates. The 600- to 615-bp fragments derived from cells transfected with DE25 (lane 4), DImA (lane 5), and DImB (lane 6) were used as templates.

teins originally identified as lying within the 87 nucleotides at positions 171–85 upstream from the 3′ end of the MHV genome (Yu and Leibowitz, 1995a). A series of RNAs containing deletions or transversion mutations within this region were tested for their ability to bind host cell proteins. These experiments mapped the protein binding element to a 38-nucleotide sequence spanning positions 166–129 upstream from the 3′ end of the MHV genome. To determine the possible role of this element in viral replication, a series of deletion mutant DI RNAs were constructed. The data we presented here revealed that sequences within the 154–129 element are necessary for RNA replication.

Several lines of evidence have demonstrated specific binding of host proteins to the 3′ end of positive-strand virus genomic RNA. For hepatitis A virus, host cell proteins with molecular masses of 38, 45, 57, and 84 kDa, specifically interact not only with the 3′-UTR of the HAV genome but also with sequences preceding the 3′-UTR and extending into the 3D^{pol}-coding region (Kusov *et al.,* 1996). For West Nile encephalitis virus, a flavivirus, 84- and 105-kDa cell proteins bind specifically to the 3′-

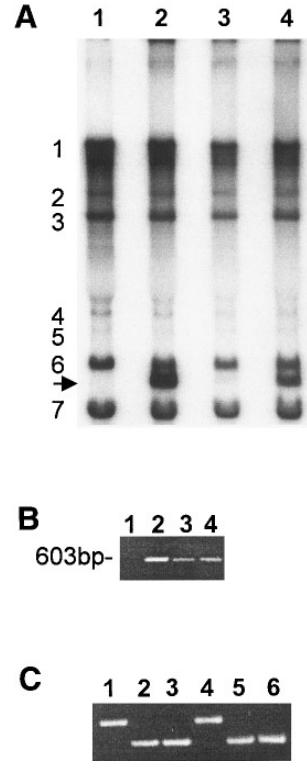

FIG. 6. Replication of wild-type DE25 and DE25-derived mutants DImC and DImD in MHV-JHM-infected 17CL-1 cells. Transfection of DI RNA and the analysis of DI RNA synthesis were performed as described in the legend of Fig. 5. (A) Metabolically labeled RNA was displayed by gel electrophoresis. Lane 1, MHV-JHM-infected intracellular RNA without transfected DI RNA; lane 2, transfected with DE25; lane 3, transfected with DImC; lane 4, transfected with DImD. (B) Negative strand DI RNA was analyzed by RT-PCR as described in the legend to Fig. 5. Lane numbers correspond to the same samples as for A. A ΦX174 DNA/HaeIII fragment was used as a 603-bp size marker. The amplified DNA fragments around 600–615 bp shown in B were recovered and used as templates for the amplification of smaller fragments containing the mutagenized regions in the input DI RNAs. The plasmids used for transcription of wild-type and mutant DI RNAs were also used as templates for nested PCR to provide size markers for the expected wild-type and mutant sequences. PCR products were resolved by 3.5% Metaphor agarose gel electrophoresis. Lanes 1, 2, and 3, plasmids DE25, mC, and mD, respectively, were used as templates. The 600- to 615-bp fragments derived from cells transfected with DE25 (lane 4), DImC (lane 5), and DImD (lane 6) were used as templates.

terminal stem–loop RNA (Blackwell *et al.,* 1995). Similar RNA–host protein interactions at the 3′ end of positive-strand RNA also have been demonstrated for mouse hepatitis virus (Yu and Leibowitz, 1995a), rhinovirus (Todd *et al.,* 1995), and rubella virus (Nakhasi *et al.,* 1990). Specific host–protein interactions with cis-acting terminal elements of RNA viruses may be required for viral RNA replication. The association of host proteins with RNA-dependent RNA polymerase has been shown for poliovirus and brome mosaic virus (Andino *et al.,* 1990, 1993; Quadt *et al.,* 1993). However, in most cases the identity and function of the host proteins binding viral RNAs remains unknown.

RNA sequence elements with protein binding activities often contain extensive secondary structure (Blackwell *et al.,* 1995; Dildine and Semler, 1992; Nakhasi *et al.,* 1991). The specific binding of alfalfa mosaic virus coat protein to viral RNA requires a combination of sequence and structural determinants located at the 3′ end of the viral RNAs (Houser-Scott *et al.,* 1994). We hypothesize that the secondary structure of the protein binding element between nucleotides 166 and 129 upstream from the 3′ end of the MHV genome is involved in the formation of RNA–protein complexes. This is suggested by the theoretical secondary structures of wild-type RNA probe 166–85 (containing the nt 166–129 element) and the deletion mutants (deleted at nt 166–155, nt 154–140, nt 139–129 and nt 128–118) used in our RNA–protein binding assays (Fig. 7). Each RNA is predicted to contain two stem–loops and at least two bulges. A small bulge containing the three nucleotides UGA, either derived from the conserved 11-nt motif UGAGAGAAGUU (nt 139–129), or from the rearrangement of adjacent nucleotides (mB), may be important for host protein binding. The mA deletion mutant which disrupts this small bulge has greatly diminished binding ability. The same three nucleotides (UGA) within the conserved 11-nt motif (UGAAUGAAGUU) in the more downstream 3′ (+) 42 element also seems to play an important role in RNA–protein interactions and is predicted to form a bulge in at least some probes which are active in RNA binding assays (Yu and Leibowitz, 1995b). However, not all probes containing this protein binding element are predicted to contain this UGA bulge. Among three clustered-point transversion mutants, mB_4 (UGA → AUG), mJ (AU → UA), and mC_5 (GAAGUU → CUUCAA) created within the conserved 11-nt sequence (UGAAUGAAGUU) in the 3′(+) 42 protein binding element, the mutation of UGA sequence in mB_4 has the greatest effect on the formation of RNA–protein complexes, only exhibiting 37% of wild-type RNA–protein binding activity, compared to 58 and 88% of wild-type RNA–protein binding activity with the mutation of AU (mJ) and GAAGUU (mC_5). Biochemical determinations of secondary structure and further mutagenic studies are needed to test our hypothesis.

MHV RNA genomes recombine at high frequency (Baric *et al.,* 1990; Lai *et al.,* 1985; Makino *et al.,* 1986b), including recombination between transfected DI RNA and helper virus genomes (de Groot *et al.,* 1994; Furuya *et al.,* 1993; van der Most *et al.,* 1992). There is one report of recombination between coronavirus RNA and transfected nonreplicating RNA fragments (Liao and Lai, 1992). RNA recombination events complicate extending the results of mutational analyses of the protein binding element to DI RNA replication. The inability of agarose gel electrophoresis of metabolically labeled intracellular RNA to distinguish between mutant DI RNA and DI RNAs containing the wild-type sequence limits this technique's usefulness. Recombination may occur at different times after transfection. Thus differences in the timing of a recombination event converting mutant to wild type could account for experiment to experiment variability in the replication level of a single mutant DI RNA observed by this technique (Yu and Leibowitz, 1995b, this work). Similarly, differences in the timing of recombination events generating wild-type DI RNAs among separate transfections with different mutants make quantitative comparisons of these mutants difficult to interpret unless the status of the mutation within the replicating molecules has been determined. The nested RT-PCR analyses provide these data and also give an independent estimate of the relative levels of replicating mutant DI and wild-type DI RNAs present within a single culture.

Both DImA and DImB were almost completely converted to wild-type DI in three separate and independent experiments, complicating the interpretation of the results. However, it is clear that both of these mutant DIs are at a severe replicative disadvantage relative to RNA molecules with the wild-type sequence (Fig. 5C). It seems likely that the rapid and reproducible replacement of the input mutant DImA and DImB RNAs by wild-type recombinants reflects a very low replication efficiency for these mutants, suggesting that most of the DI RNA detected in the metabolic labeling assays are likely wild-type DI. These same deletion mutations also decrease protein binding activity to 4 (mA) and 37% (mB) of those observed with the wild-type sequence. In three separate experiments, we failed to detect metabolically labeled positive strand DImB, which contains a deletion of the 11-nt motif UGAGAGAAGUU. However, PCR analyses demonstrated that synthesis of mutant negative strand RNAs did take place, although the amount of negative strand RNA appeared to be reduced relative to DE25. One possible explanation for these disparate results relates to differences in the timing or frequency of recombination events of these two DI RNAs with helper virus combined with differences in the relative sensitivity of the methods used to detect positive and negative strand progeny RNA. Alternatively, deletion of this sequence could primarily affect positive strand synthesis. These two explanations are not mutually exclusive and both could contribute to the observed results.

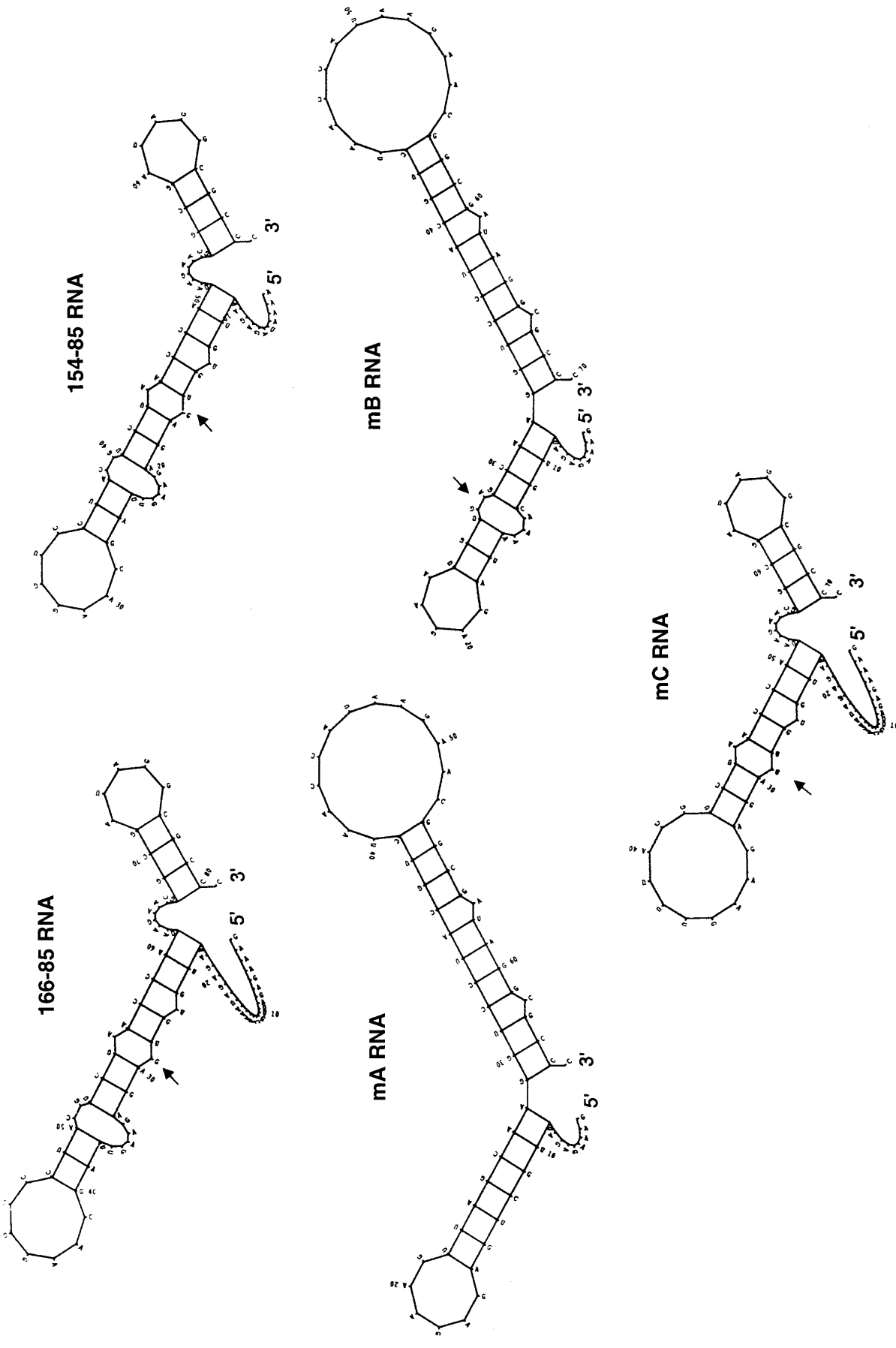

FIG. 7. Secondary structure predictions of wild-type 166–85 RNA and 166–85-derived deletion mutants. Secondary structures were predicted by the Fold program in the University of Wisconsin Genetics Computer Group sequence analysis package. The structures depicted are for the same RNAs described in Fig. 1. Arrows indicate bulges containing UGA.

Recombination of DImC and DImD with the helper virus was not detected in three independent experiments, thus for these mutants the interpretation of the metabolic labeling experiments is relatively straight forward. The mutation in DImD, which has no effect on protein binding (Fig. 1A), has a modest effect on positive strand RNA replication, decreasing replication to about half that observed with wild-type DI RNA. The mutation in DImC, which has a minimal effect on protein binding (Fig. 1B) had a more severe effect on positive strand replication, with DImC only achieving 4–8% of the levels observed with wild-type DI RNAs. The differential effects of these two mutants on virus replication are likely at the level of positive strand synthesis, since the RT-PCR results, although not quantitative, suggest that there is no great disparity in the amount of negative strand template produced by these two DI RNAs. These data are consistent with previous results, suggesting that sequences from 436–56 upstream from the 3′ end of the genome have a role in positive strand RNA replication (Kim *et al.,* 1993; Lin *et al.,* 1994).

Taken together, the data from all of the transfection experiments suggest several conclusions. First, the metabolic labeling experiments suggest that the relative ability of the DImD and DImC mutants to replicate is DImD $>$ DImC. Second, the inability of DImA and DImB to compete with wild-type recombinants, which arise during the replicative cycle, while the DImD and DImC mutants are able to be maintained, suggests that the relative ability of the four mutants to replicate is DImD $>$ DImC $>$ DImB and DImA. Thus replicative ability parallels the relative protein binding activity of probes containing these different mutations, although the absolute effects of mutations on these two activities is different. These data are consistent with the notion that sequences between nt 166 and 129 are involved in viral replication and protein binding, and that these two activities might be linked. Further mutagenic and structural studies of this element and identification of the proteins which recognize this sequence are needed to critically test this hypothesis. Third, sequences within the 166–129 element (nt 154–129) provide necessary functions for replication. Based on previously published work (Lin *et al.,* 1994) and our findings discussed above, we suspect that these functions are primarily required for positive strand synthesis. Lin *et al.* (1994) have shown that the minimum cis-acting signal for MHV minus-strand RNA synthesis is contained within the last 55 nt plus the poly(A) tail at the 3′ end of MHV genome. The 166–129 protein binding element is upstream of the 55 nucleotides required for negative strand synthesis, but is within the 436-nt sequence at the 3′ end of the genome which is required for DI replication (Kim *et al.,* 1993; Lin and Lai, 1993).

In this work the protein complexes recognizing the 166–129 protein binding element have been partially characterized by UV cross-linking studies. We have identified a polypeptide of approximately 120 kDa, two polypeptides between 55 and 50 kDa, two polypeptides approximately 40 kDa, and a polypeptide of approximately 25 kDa molecular mass. Previous studies using a larger probe (487–85) encompassing this binding element labeled five host polypeptides 142, 120, 100, 55, and 33 kDa in size, with the 120-kDa protein being the most heavily labeled protein component in the complex (Yu and Leibowitz, 1995a). However, additional faint and indistinct bands were also sometimes observed, including bands similar in size to the 40- and 25-kDa polypeptides we report here. Thus, these two studies are largely consistent, although the 142- and 100-kDa polypeptides detected with the larger probe were not detected in the current set of experiments, suggesting that these polypeptides might interact with an additional protein binding element further upstream. Additional protein binding elements have been identified within the 5′ and 3′ termini of the MHV genome (Furuya and Lai, 1993; Yu and Leibowitz, 1995a). Investigations of the 3′(+)42 element very near the 3′ end of the genome have demonstrated that this element also binds 120- and 55-kDa host proteins, and that disruption of this element by mutation has a deleterious effect on replication (Yu and Leibowitz, 1995a, 1995b). A study of protein binding to the 5′ end of the MHV genome has demonstrated binding of a 55-kDa host cell protein to positive sense RNA corresponding to nt 56–112 at the 5′ end of the viral genome (Furuya and Lai, 1993). More detailed studies are needed to determine if the same 55-kDa protein binds to all three protein binding elements.

ACKNOWLEDGMENTS

We thank all members of Dr. Leibowitz's laboratory for helpful discussions. This work was supported in part by National Multiple Sclerosis Society Research Grants RG 2203-A-5 and RG 2203-B-6. Q. Liu thanks the WHO for providing the opportunity to study in Dr. Leibowitz's laboratory.

REFERENCES

Andino, R., Rieckhof, G. E., and Baltimore, D. (1990). A functional ribonucleoprotein complex forms around the 5′ end of poliovirus RNA. *Cell* 63, 369–380.

Andino, R., Rieckhof, G. E., Achacoso, P. L., and Baltimore, D. (1993). Poliovirus RNA synthesis utilizes an RNP complex formed around the 5′ end of viral RNA. *EMBO J.* 12, 3587–3598.

Baric, R. S., Fu, K., Schaad, M. C., and Stohlman, S. A. (1990). Establishing a genetic recombination map for MHV-A59 complementation groups. *Virology* 177, 646–656.

Brian, D. A., Chang, R. Y., Hofmann, M. A., and Sethna, P. B. (1994). Role of subgenomic minus-strand RNA in coronavirus replication. *Arch. Virol. (Suppl.)* 9, 173–180.

de Groot, R., Heijnen, L., van der Most, R. G., and Spaan, W. (1994). Homologous RNA recombination allows efficient introduction of site-specific mutations into the genome of coronavirus MHV-A59 via synthetic co-replicating RNAs. *Arch. Virol. (Suppl.)* 9, 221–230.

Blackwell, J. L., and Brinton, M. A. (1995). BHK cell proteins that bind to the 3′ stem-loop structure of the west nile virus genome RNA. *J. Virol.* 69, 5650–5658.

Dildine, S. L., and Semler, B. L. (1992). Conservation of RNA-protein interactions among picornaviruses. *J. Virol.* 66, 4364–4376.

Furuya, T., and Lai, M. M. C. (1993). Three different cellular proteins bind to complementary sites on the 5′-end positive and 3′-end negative strands of mouse hepatitis virus RNA. *J. Virol.* 67, 7215–7222.

Furuya, T., Macnaughton, T. B., Monica, N. L., and Lai, M. M. C. (1993). Natural evolution of coronavirus defective-interfering RNA involves RNA recombination. *Virology* 194, 408–413.

Houser-Scott, F., Baer, M. L., Liem, K. F., Jr., Cai, J. M., and Gehrke, L. (1994). Nucleotide sequence and structural determinants of specific binding of coat protein or coat protein peptides to the 3′ untranslated region of alfalfa mosaic virus RNA 4. *J. Virol.* 68, 2194–2205.

Kim, Y. N., Jeong, Y. S., and Makino, S. (1993). Analysis of cis-acting sequence essential for coronavirus defective interfering RNA replication. *Virology* 197, 53–63.

Kim, Y. N., and Makino, S. (1995). Characterization of a murine coronavirus defective interfering RNA internal cis-acting replication signal. *J. Virol.* 69, 4963–4971.

Kusov, Y., Weitz, M., Dollenmeier, G., Gauss-Muller, V., and Siegl, G. (1996). RNA-protein interactions at the 3′ end of the Hepatitis A virus RNA. *J. Virol.* 70, 1890–1897.

Lai, M. M. C. (1990). Coronavirus: Organization, replication and expression of genome. *Annu. Rev. Microbiol.* 44, 303–333.

Lai, M. M. C., Baric, R. S., Brayton, P. R., and Stohlman, S. A. (1984). Characterization of leader RNA sequences on the virion and mRNAs of mouse hepatitis virus, a cytoplasmic RNA virus. *Proc. Natl. Acad. Sci. USA* 81, 3626–3630.

Lai, M. M. C., Baric, R. S., Makino, S., Keck, J. C., Egbert, J., Leibowitz, J. L., and Stohlman, S. A. (1985). Recombination between nonsegmented RNA genomes of murine coronavirus. *J. Virol.* 56, 449–456.

Lai, M. M. C., and Stohlman, S. A. (1978). RNA of mouse hepatitis virus. *J. Virol.* 26, 236–242.

Liao, C. L., and Lai, M. M. C. (1992). RNA recombination in a coronavirus: recombination between viral genomic RNA and transfected RNA fragments. *J. Virol.* 66, 6117–6124.

Lee, H. J., Shieh, C. K., Gorbalenya, A. E., Koonnin, E. V., La Monica, N., Tuler, J., Bagdzhadzhyan, A., and Lai, M. M. C. (1991). The complete sequence (22 kilobases) of murine coronavirus gene 1 encoding the putative proteases and RNA polymerase. *Virology* 180, 567–582.

Leibowitz, J. L., Wilhelmsen, K. C., and Bond, C. W. (1981). The virus specific intracellular RNA species of two murine coronaviruses: MHV-A59 and MHV-JHM. *Virology* 114, 39–51.

Leibowitz, J. L., Zoltick, P. W., Holmes, K. V., Oleszak, E. L., and Weiss, S. R. (1990). Murine coronavirus RNA synthesis. *In* "New Aspects of Positive-Strand RNA Virus" (M. A. Brinton and F. X. Heinz, Eds.), pp. 67–74. Am. Soc. Microbiol. Washington, DC.

Lin, Y. J., and Lai, M. M. C. (1993). Deletion mapping of a mouse hepatitis virus defective interfering RNA reveals the requirement for an internal and discontinuous sequence for replication. *J. Virol.* 67, 6110–6118.

Lin, Y. J., Liao, C. L., and Lai, M. M. C. (1994). Identification of the cis-acting signal for minus-strand RNA synthesis of a murine coronavirus: Implications for the role of minus-strand RNA in RNA replication and transcription. *J. Virol.* 68, 8131–8140.

Makino, S., Joo, M., and Makino, J. K. (1991). A system for study of coronavirus mRNA synthesis: A regulated, expressed subgenomic defective interfering RNA results from intergenic site insertion. *J. Virol.* 65, 6031–6041.

Makino, S., Keck, J. G., Stohlman, S. A., and Lai, M. M. C. (1986b). High-frequency RNA recombination of murine coronaviruses. *J. Virol.* 57, 729–737.

Makino, S., and Lai, M. M. C. (1989). High-frequency leader sequence switching during coronavirus defective interfering RNA replication. *J. Virol.* 63, 5285–5292.

Makino, S., Shieh, C. K., Soe, L. H., Baker, S. C., and Lai, M. M. C. (1988). Primary structure and translation of a defective interfering RNA of murine coronavirus. *Virology* 166, 550–560.

Nakhasi, H. L., Cao, X. Q., Rouault, T. A., and Lui, T. Y. (1991). Specific binding of host cell proteins to the 3′-terminal stem-loop structure of rubella virus negative-strand RNA. *J. Virol.* 65, 5961–5967.

Nakhasi, H. L., Rouault, T. A., Haile, D. J., Liu, T. Y., and Klausner, R. D. (1990). Specific high-affinity binding of host cell proteins to the 3′ region of rubella virus RNA. *New Biol.* 2, 255–264.

Pachuk, C. J., Bredenbeek, P. J., Zoltick, P. W., Spaan, W. J. M., and Weiss, S. R. (1989). Molecular cloning of the gene encoding the putative polymerase of mouse hepatitis coronavirus strain A59. *Virology* 171, 141–148.

Parker, M. M., and Masters, P. S. (1990). Sequence comparison of the N genes of five strains of the coronavirus mouse hepatitis virus suggests a three domain structure for the nucleocapsid protein. *Virology* 179, 463–468.

Quadt, R., Kao, C. C., Browning, K. S., Hershberger, R. P., and Ahlquist, P. (1993). Characterization of a host protein associated with brome mosaic virus RNA-dependent RNA polymerase. *Proc. Natl. Acad. Sci. USA* 90, 1498–1502.

Sawicki, S. G., and Sawicki, D. L. (1990). Coronavirus transcription: Subgenomic mouse hepatitis virus replicative intermediates function in RNA synthesis. *J. Virol.* 64, 1050–1056.

Sethna, P. B., Hung, S. L., and Brian, D. A. (1989). Coronavirus subgenomic minus-strand RNAs and the potential for mRNA replicons. *Proc. Natl. Acad. Sci. USA* 86, 5626–5630.

Siddell, S. G., Wege, H., and ter Meulen, V. (1983). The biology of coronaviruses. *J. Gen. Virol.* 64, 761–776.

Spaan, W. J., Rottier, P. J., Horzinek, M. C., and van der Zeijst, B. A. M. (1981). Isolation and identification of virus-specific mRNAs in cells infected with mouse hepatitis virus (MHV-A59). *Virology* 108, 424–434.

Todd, S., Nguyen, J. H. C., and Semler, B. L. (1995). RNA-protein interactions directed by the 3′ end of human rhinovirus genomic RNA. *J. Virol.* 69, 3605–3614.

van der Most, R. G., Heijnen, L., Spaan, J. M., and de Groot, R. J. (1992). Homologous RNA recombination allows efficient introduction of site-specific mutations into the genome of coronavirus MHV-A59 via synthetic co-replicating RNA. *Nucleic Acids Res.* 20, 3357–3371.

Wege, H., Siddell, S. G., and ter Meulen, V. (1982). The biology and pathogenesis of coronaviruses. *Curr. Top. Microbiol. Immunol.* 99, 165–200.

Yu, W., and Leibowitz, J. L. (1995a). Specific binding of host cellular proteins to multiple sites within the 3′ end of mouse hepatitis virus genomic RNA. *J. Virol.* 69, 2016–2023.

Yu, W., and Leibowitz, J. L. (1995b). A conserved motif at the 3′ end of mouse hepatitis virus genomic RNA required for host protein binding and viral RNA replication. *Virology* 214, 128–138.